Title page

C-type natriuretic peptide improves maternally aged oocytes quality by inhibiting excessive PINK1/Parkin-mediated mitophagy

Running title: CNP improves oocytes quality

Hui Zhang[1, 2a], Chan Li[1, 2a], Qingyang Liu[1, 2], Jingmei Li[1, 2], Hao Wu[1, 2], Rui Xu[1, 2], Yidan Sun[1, 2], Ming Cheng[1, 2], Xiaoe Zhao[1, 2], Menghao Pan[1, 2], Qiang Wei[1, 2b], Baohua Ma[1, 2b]

1 College of Veterinary Medicine, Northwest A&F University, Yangling, Shaanxi, People's Republic of China,

2 Key Laboratory of Animal Biotechnology, Ministry of Agriculture, Yangling, Shaanxi, People's Republic of China

[a] These authors contributed equally.

[b] Corresponding author: Baohua Ma and Qiang Wei

Address: College of Veterinary Medicine, Northwest A&F University, Yangling, Shaanxi, People's Republic of China; Key Laboratory of Animal Biotechnology, Ministry of Agriculture, Yangling, Shaanxi, People's Republic of China. 712100

Email: mabh@nwsuaf.edu.cn (Baohua Ma); weiq@nwsuaf.edu.cn (Qiang Wei).

Abstract

The overall oocyte quality declines with ageing, and this effect is strongly associated with a higher reactive oxygen species (ROS) level and the resultant oxidative damage. C-type natriuretic peptide (CNP) is a well-characterized physiological meiotic inhibitor that has been successfully used to improve immature oocyte quality during in vitro maturation (IVM). However, the underlying roles of CNP in maternally aged oocytes have not been reported. Here, we found that the age-related reduction in the serum CNP concentration was highly correlated with decreased oocyte quality. Treatment with exogenous CNP promoted follicle growth and ovulation in aged mice and enhanced meiotic competency and fertilization ability. Interestingly, the cytoplasmic maturation of aged oocytes was thoroughly improved by CNP treatment, as assessed by spindle/chromosome morphology and redistribution of organelles (mitochondria, the endoplasmic reticulum [ER], cortical granules [CGs], and the Golgi apparatus). CNP treatment also ameliorated DNA damage and apoptosis caused by ROS accumulation in aged oocytes. Importantly, oocyte RNA-seq revealed that the beneficial effect of CNP on aged oocytes was mediated by restoration of mitochondrial oxidative phosphorylation, eliminating excessive mitophagy. CNP reversed the defective phenotypes in aged oocytes by alleviating oxidative damage and suppressing excessive PINK1/Parkin-mediated mitophagy. Mechanistically, CNP functioned as a cAMP/PKA pathway modulator to decrease PINK1 stability and

inhibit Parkin recruitment. In summary, our results demonstrated that CNP supplementation constitutes an alternative therapeutic approach for advanced maternal age-related oocyte deterioration and may improve the overall success rates of clinically assisted reproduction in older women.

Keywords: C-type natriuretic peptide; oocyte meiosis; embryo; antioxidant; mitophagy

INTRODUCTION

During growth, oocytes gradually acquire the capacity to resume meiosis, complete maturation, undergo successful fertilization and achieve subsequent embryo developmental competence (Gandolfi & Gandolfi, 2001). However, ovarian involution precedes that of any other organ in female mammals, and in humans, the oocyte fertilization rate decreases rapidly after 35 years of age. Indeed, infertility associated with a decline in oocyte quality with increasing maternal age is a significant challenge.

Recently, with the development of cultural and social trends, many women have delayed childbearing, and ovarian senescence has become a public health problem (Bartimaeus, Obi, Igwe, & Nwachuku, 2020; Broekmans, Soules, & Fauser, 2009). Ovarian ageing is accompanied by abnormalities in organelle distribution, morphology and functions, leading to inadequate oocyte growth, maturation, fertilization and subsequent embryo development (Reader, Stanton, & Juengel, 2017). Consequently, assisted reproductive technologies such as in vitro maturation (IVM)

64 and in vitro fertilization (IVF) have become promising options for infertility treatment
65 (Chang, Song, Lee, Lee, & Yoon, 2014). However, further studies are needed to
66 improve the subsequent developmental competence of maternally aged oocytes.

67 Oocyte maturation has two steps: nuclear maturation, which mainly involves
68 germinal vesicle breakdown (GVBD) and chromosomal segregation, and cytoplasmic
69 maturation, which involves redistribution of organelles (mitochondria, cortical
70 granules [CGs], and the endoplasmic reticulum [ER]), changes in the intracellular
71 ATP and antioxidant contents, and the accumulation of fertilization-related transcripts
72 and proteins (McClatchie et al., 2017; Watson, 2007). The quality and developmental
73 potential of aged oocytes are lower than those of oocytes derived from young females,
74 primarily because aged oocytes exhibit negative consequences of cytoplasmic
75 maturation, such as abnormal mitochondria and an aberrant CG distribution (Miao,
76 Cui, Gao, Rui, & Xiong, 2020), deteriorated organelle and antioxidant system
77 function and increased reactive oxygen species (ROS) levels (T. Zhang et al., 2019).
78 Excessive ROS generation leads to destructive effects on cellular components
79 (Zarkovic, 2020). Notably, recent studies have indicated that increased oxidative
80 damage is closely correlated with the occurrence of mitochondrial damage and
81 mitophagy (Jiang et al., 2021), which is accompanied by blockade of oocyte meiosis
82 (Jin et al., 2022; Q. Shen, Liu, Li, & Zhang, 2021).

83 The endogenous C-type natriuretic peptide (CNP) produced by follicular mural
84 granulosa cells as a ligand of natriuretic peptide receptor 2 (NPR2), which is

85 expressed primarily in cumulus cells, plays a crucial role in maintaining meiotic arrest
86 (Meijia Zhang, Su, Sugiura, Xia, & Eppig, 2010). Recent studies have suggested that
87 CNP, an inhibitor of oocyte maturation, provides adequate time for cytoplasmic
88 maturation, offering a new strategy to optimize the synchronization of nuclear and
89 cytoplasmic maturation and improve the quality of immature oocytes in vitro (Wei et
90 al., 2017). Moreover, CNP has been reported to enhance the antioxidant defence
91 ability and developmental competence of oocytes in vitro (Zhenwei & Xianhua, 2019).
92 Therefore, CNP may constitute a new alternative means to enhance antioxidant
93 system function and protect against oxidative damage by eliminating excess ROS in
94 aged oocytes. Although CNP has been suggested to contribute to improving the
95 maturation and subsequent development of immature mouse oocytes in vitro, the
96 effect of CNP on maternally aged oocytes remains to be determined.

97 In this study, we investigated the redistribution and function of organelles
98 (mitochondria, CGs, and the ER), the ATP content and the intracellular GSH level in
99 CNP-treated maternally aged oocytes. The results showed that CNP improves the
100 cytoplasmic maturation and developmental competence of maternally aged oocytes by
101 optimizing organelle distribution and function and inhibiting PINK1/Parkin-mediated
102 mitophagy. The findings of this study will contribute to understanding the mechanism
103 of CNP in increasing the fertilization capacity and developmental ability of aged
104 oocytes.

105 **RESULTS**

106 **CNP supplementation improves the quality of aged oocytes**

107 To explore the effect of CNP on oocyte quality in aged mice, we first
108 investigated whether intraperitoneal injection of CNP can affect oocyte quality. Young
109 and aged mice were hormonally superovulated after 14 days of consecutive PBS or
110 CNP treatment (Figure 1A, B). Then, the mice were sacrificed, and the oocytes were
111 removed for measurement of the CNP content. As expected, the endogenous CNP
112 content in serum from aged mice was markedly lower than that in serum from young
113 mice (Figure 1 C). In contrast, administration of CNP to aged mice significantly
114 elevated the CNP content in serum (Figure 1 C). To further determine whether the
115 elevated CNP content in serum can improve oocyte quality, we evaluated the number,
116 first polar body (PB1) extrusion rate and fragmentation rate. As the mice aged, the
117 number of ovulations and the PB1 extrusion rate decreased significantly, but the
118 incidence of fragmented oocytes increased dramatically (Figure 1 D-G). Conversely,
119 CNP supplementation apparently ameliorated the ageing-induced defects in the
120 number and morphology of the ovulated oocytes (Figure 1 D-G). In addition,
121 assessment of follicle development in the ovary sections by HE staining showed
122 severe deterioration of follicles at different developmental stages in aged mice;
123 however, CNP supplementation significantly increased the number of secondary
124 follicles and antral follicles (Figure 1H and I). Young, untreated aged and CNP-treated
125 aged mice were naturally mated with 12-week-old male mice, and consistent with the
126 increased number of ovulated oocytes with a normal morphology, the litter size of

127 aged mice was also increased by CNP administration (Figure 1J).

128 To investigate the effects of CNP on in vitro maturation (IVM) of aged mouse
129 cumulus-oocyte complexes (COCs), we first examined the PB1 extrusion rate of
130 COCs pretreated with 10 nM CNP to maintain meiotic arrest for 24 h (pre-IVM) and
131 then matured in vitro for 16 h (a two-step culture system; Figure S1 A). In the control
132 (conventional in vitro maturation) group, only 35.36 ± 2.74% of the oocytes exhibited
133 PB1 extrusion. After temporary meiotic arrest induced by treatment with 10 nM CNP,
134 the maturation rate increased to 71.12 ± 3.02% (n=104), significantly higher than that
135 in the control group ($P<0.01$) (Figure S1 B and C). The spindle morphology and
136 chromosome alignment in in vitro-matured oocytes were also evaluated. The
137 percentage of oocytes with abnormal spindle-chromosome complexes was
138 significantly decreased in the group with 10 nM CNP-induced temporary meiotic
139 arrest (Figure S1 D and E). Collectively, these results indicate that CNP
140 administration increased the serum CNP content, restored the number and
141 morphology of aged oocytes and improved the fertility of aged female mice.

142 **CNP supplementation restores cytoplasmic maturation events in maternally aged**
143 **mouse oocytes**

144 Pregnancy failure and foetal miscarriage increase with maternal age and,
145 importantly, are associated with oocyte aneuploidy and spindle/chromosomal
146 abnormalities (Ma et al., 2020). Therefore, we determined the rate of
147 spindle/chromosomal abnormalities in oocytes of young, untreated aged and CNP-

148 treated aged mice by immunofluorescence staining and found that CNP treatment
149 greatly improved the spindle/chromosomal abnormalities in aged mice (Figure 2A, B).
150 To determine whether, in addition to affecting spindles/chromosomes, CNP
151 supplementation affects other organelles during the maturation of aged oocytes, we
152 examined the distribution of the Golgi apparatus, endoplasmic reticulum (ER) and
153 cortical granules (CGs) in oocytes from young, untreated aged and CNP-treated aged
154 mice. The Golgi-Tracker results showed that in aged mouse oocytes, the Golgi
155 apparatus was distributed in agglutinated and clustered patterns, and CNP
156 supplementation significantly reduced the rate of abnormal Golgi distribution (Figure
157 2 C, D, Figure S2A, B). Since the ER plays an essential role in Ca^{2+} signal-mediated
158 oocyte fertilization and subsequent embryonic development (Miyazaki & Ito, 2006),
159 we then examined the distribution pattern of the ER in oocytes. As shown in Figure
160 2E, the ER was accumulated at the chromosome periphery and was evenly distributed
161 in the cytoplasm; however, the ER abnormally agglomerated in the cytoplasm and the
162 chromosome periphery in a disorganized pattern in aged oocytes (Figure 2E, Figure
163 S3A). Statistical analysis showed that the rate of abnormal ER distribution was
164 significantly decreased in CNP-supplemented oocytes (Figure 2F, Figure S3B). The
165 distribution of CGs is one of the most important indicators of oocyte cytoplasmic
166 maturation and is related to the blockade of polyspermy following fertilization. We
167 assessed whether CNP supplementation affects the distribution dynamics of CGs in
168 aged oocytes. Lens culinaris agglutinin (LCA)-FITC staining showed that in young

169 oocytes, CGs were distributed evenly in the oocyte subcortical region, leaving a CG-
170 free domain (CGFD) near chromosomes (Figure 2G). However, maternally aged
171 oocytes showed an abnormal CG distribution, including increased migration of CGs
172 towards the oocyte chromosomes or oocyte subcortical region, without leaving a
173 CGFD (Figure 2G, H; Figure S4 A). Consistent with this finding, statistical analysis of
174 the fluorescence intensity of CG signals in aged oocytes showed a significant
175 reduction compared with that in young oocytes, and CNP supplementation rescued the
176 mislocalization and decrease in the number of oocyte CGs (Figure 2 H, I, Figure S4 B,
177 C). Taken together, these data imply that CNP is a potent agent for rescuing
178 cytoplasmic maturation events in maternally aged mouse oocytes.

179 **CNP supplementation restores mitochondrial distribution and function in aged**
180 **oocytes**

181 To verify the effect of CNP supplementation on the mitochondrial distribution
182 pattern and function in aged oocytes, we performed MitoTracker staining. In young
183 oocytes, mitochondria exhibited a homogeneous distribution in the cytoplasm and
184 accumulated at the periphery of chromosomes (Figure 2J). However, in aged oocytes,
185 most mitochondria were aggregated in the cytoplasm and partially or completely
186 failed to accumulate around chromosomes (Figure 2JA, Figure S5A). Statistically,
187 more than 40% of mitochondria in aged oocytes exhibited a mislocalized distribution
188 pattern, and CNP supplementation significantly reduced the abnormal distribution rate
189 (Figure 2K, Figure S5B). We then analysed mitochondrial function by measuring the

190 ATP content in oocytes from young, untreated aged, and CNP-treated aged mice. The
191 ATP content in oocytes from aged mice was considerably lower than that in oocytes
192 from young mice but was restored following CNP supplementation (Figure 2L, Figure
193 S5C). We also tested the mitochondrial membrane potential, which has been shown to
194 be the driving force of mitochondrial ATP synthesis, by staining with the
195 potentiometric dye JC-1 (Figure 2M, Figure S5D). The mitochondrial membrane
196 potential was lower in oocytes from aged mice than in oocytes from young mice but
197 was restored in oocytes from CNP-supplemented aged mice (Figure 2M, N, Figure
198 S5D, S5E). Overall, these observations suggest that CNP supplementation improved
199 ageing-induced mitochondrial dysfunction in oocytes.

200 **CNP supplementation eliminates excessive ROS and attenuates DNA damage**
201 **and apoptosis in aged oocytes**

202 We proposed that mitochondrial dysfunction induces ROS imbalance and
203 oxidative stress in aged oocytes. To test this hypothesis, we carried out
204 dichlorofluorescein (DCFH) staining to measure ROS levels in each group of oocytes
205 (Figure 3A). Quantitative analysis of the fluorescence intensity showed that ROS
206 signals were markedly enhanced in aged oocytes compared with young oocytes
207 (Figure 3B). Conversely, CNP supplementation effectively reduced the ROS
208 accumulation observed in aged oocytes (Figure 3A and 3B, Figure S6A, S6B). In
209 addition to being caused by ROS accumulation, age-associated oxidative stress
210 damage can be caused by reduced antioxidant defence system function. We therefore

211 investigated whether CNP contributes to improving the antioxidant defence ability in
212 aged oocytes. Quantification of the nicotinamide adenine dinucleotide phosphate
213 (NADPH) levels and the ratio of reduced to oxidized glutathione (GSH/GSSG ratio)
214 in oocytes showed that NADPH levels and the GSH/GSSG ratio were decreased in
215 oocytes from aged mice compared with those from young mice and that CNP
216 treatment significantly increased NADPH levels and the GSH/GSSG ratio in oocytes
217 from aged animals (Figure 3C and 3D). Because a high level of ROS not only results
218 in the accumulation of DNA damage but also causes oocyte apoptosis (Miao et al.,
219 2020), we next evaluated DNA damage and apoptosis in oocytes by γ-H2A.X and
220 Annexin-V staining, respectively. As expected, higher signals indicating DNA damage
221 and apoptosis were observed in aged oocytes than in young oocytes, and these
222 increases were alleviated by supplementation with CNP (Figure 3E-3H). Taken
223 together, these observations suggested that the rates of DNA damage and apoptosis
224 are higher in aged oocytes, possibly because of maternal ageing-induced excessive
225 accumulation of ROS. Notably, our results demonstrated that CNP supplementation
226 exerts antioxidant activity, which is an effective strategy to ameliorate maternal
227 ageing-induced DNA damage and apoptosis in oocytes.

228 **CNP supplementation improves the fertilization ability and early embryo**
229 **development of aged oocytes**

230 Considering that oocyte fertilization and subsequent embryo developmental
231 competence are profoundly affected by mitochondrial function, we then tested

232 whether the oocyte fertilization capacity and normal development to the blastocyst
233 stage are enhanced by CNP. The in vitro fertilization (IVF) results showed that aged
234 oocytes had dramatically lower fertilization rates than young oocytes and that CNP
235 supplementation effectively increased the fertilization rate of aged oocytes (Figure 4A,
236 B). We further examined the subsequent developmental ability of the fertilized
237 oocytes. As expected, CNP supplementation effectively increased the blastocyst
238 formation rate of aged oocytes both in vivo (Figure 4A and 4C–4F) and in vitro
239 (Figure S7). These results demonstrate that CNP increases the fertilization capacity
240 and promotes subsequent embryonic development of oocytes from aged mice.
241

242 **Identification of target effectors of CNP in aged oocytes by single-cell**
243 **transcriptome analysis**

244 To verify the cellular and molecular mechanisms of CNP supplementation in
245 improving oocyte quality in aged mice, we performed single-cell transcriptome
246 analysis of GV oocytes derived from young, untreated aged and CNP-treated aged
247 mice to identify potential target effectors. The relative expression of several randomly
248 selected genes from each group was verified using quantitative real-time PCR (Figure
249 S8A, B). As shown in the heatmap and volcano plot, the transcriptome profile of aged
250 oocytes was significantly different from that of young oocytes, with 77 differentially
251 expressed genes (DEGs) downregulated and 440 DEGs upregulated in aged oocytes
252 identified through DEGseq2 analysis (Figure 5A-C). Furthermore, CNP

253 supplementation resulted in downregulation of 584 genes and upregulation of 527
254 genes compared with aged oocytes. In particular, Kyoto Encyclopedia of Genes and
255 Genomes (KEGG) enrichment analysis showed that genes enriched in the ubiquitin-
256 mediated proteolysis and mitophagy pathways were abnormally highly expressed in
257 aged oocytes compared with young oocytes but that these expression levels were
258 restored to the baseline levels in CNP-supplemented aged oocytes (Figure 5D, E). In
259 addition, oxidative phosphorylation and peroxisome proliferator-activated receptor
260 (PPAR) signalling pathways were ranked at the top of the enrichment list in CNP-
261 supplemented aged oocytes compared to untreated aged oocytes, consistent with our
262 abovementioned observations that CNP supplementation improved mitochondrial
263 function in aged oocytes. Many of the enriched KEGG enrichment pathways are
264 highly related to mitophagy and mitochondrial function, which suggests that
265 mitophagy should be strongly considered as a CNP effector in aged oocytes.

266 **CNP supplementation attenuates oxidative damage by inhibiting mitophagy in**
267 **aged oocytes**

268 To verify the effect of CNP supplementation on mitophagy in aged oocytes, we first
269 analysed mitochondrial structure in the oocytes of young, untreated aged and CNP-
270 treated aged mice by transmission electron microscopy (Figure 6A). Quantitatively,
271 mitochondrial damage, as evidenced by membrane rupture and a lack of electron
272 density was significantly increased in aged oocytes but was ameliorated in CNP-
273 supplemented aged oocytes (Figure 6B). Because oxidative stress has been implicated

274 in triggering mitochondrial oxidative injury and mitophagy (Adhikari, Lee, Yuen, &
275 Carroll, 2022; M. Shen et al., 2016), we next determined whether supplementation
276 with CNP can eliminate excessive mitochondrial ROS (mtROS). As expected,
277 supplementation with CNP substantially reduced the mtROS signals, as shown by
278 MitoSOX staining and fluorescence intensity measurements (Figure 6 C, D). We then
279 evaluated degradation of the autophagy biomarker p62, the accumulation of LC3-II,
280 the conversion of LC3-I to LC3-II, and the expression patterns of the mitophagy-
281 related proteins PINK1 and Parkin (Figure 6 E). Western blot analysis revealed that
282 aged oocytes exhibited significant p62 degradation, LC3-II accumulation and marked
283 increases in PINK1 and Parkin expression levels, whereas CNP supplementation
284 abrogated these effects (Figure 6E-6I). Collectively, the above data indicate the
285 inhibitory effect of CNP on oocyte mitophagy through the PINK1-parkin signalling
286 pathway.

287 **CNP downregulates Parkin recruitment and mitophagy via the cAMP/PKA**
288 **pathway**

289 How PINK1- and Parkin-mediated mitophagy is regulated by CNP in aged
290 oocytes, however, requires further elucidation. The cAMP/PKA signalling pathway,
291 which is dependent on the phosphorylation of mitochondrial proteins, has emerged as
292 a direct means to regulate mitophagy and mitochondrial physiology (Amer & Hebert-
293 Chatelain, 2018; Lobo et al., 2020). The concentrations of cAMP in GV oocytes
294 derived from young, untreated aged and CNP-treated aged mice were determined. As

295 shown in Fig. 6J, the cAMP concentration in aged oocytes was significantly lower
296 than that in young oocytes, but administration of CNP resulted in a substantial
297 increase in intraoocyte cAMP concentrations. This increase in cAMP significantly
298 reduced mitochondrial recruitment of Parkin and mitophagy, which were dependent
299 on PKA activity (Lobo et al., 2020). Next, we applied a PKA inhibitor, H89, to
300 determine whether PKA is directly involved in CNP-mediated oocyte mitophagy. We
301 isolated preantral follicles (80–100 μm diameter) from the ovaries of aged mice and
302 treated them with 100 nM CNP or 100 nM CNP + 10 μM H89 during in vitro culture.
303 Monitoring of follicle growth dynamics showed that treatment with 100 nM CNP
304 significantly increased the follicle diameter (Figure 8B and C), whereas H89
305 treatment inhibited the effect of CNP on promoting preantral follicle growth (Figure 6
306 K and L). Western blot analysis revealed that CNP supplementation significantly
307 decreased PINK1 and Parkin expression levels, but H89 treatment abrogated these
308 expression changes (Figure 6 M-O). The cAMP-PKA pathway plays an important role
309 in inhibiting Parkin recruitment to damaged mitochondria (Akabane et al., 2016). We
310 therefore sought to determine whether PKA inhibition regulates Parkin recruitment.
311 The effects of CNP on mitochondria were examined by double staining for Parkin and
312 translocase of outer mitochondrial membrane 20 (TOMM20). CNP clearly inhibited
313 the mitochondrial localization of Parkin, but inhibition of PKA with H89 resulted in
314 Parkin translocation to mitochondria, as shown by the overlap of the two staining
315 signals (Figure 6 P and Q). Collectively, these data suggested that the suppression of

316 Parkin recruitment through the cAMP-PKA axis is an important mechanism
317 underlying the protective effect of CNP against oxidative injury in maternally aged
318 mouse oocytes.

319 **DISCUSSION**

320 In mammals, the endogenous peptide CNP is expressed by endothelial cells in
321 many tissues and has diverse physiological functions in mediating cardioprotective
322 effects, bone growth, oocyte meiotic progression, and follicle growth and
323 development (Bae et al., 2017; Moyes & Hobbs, 2019; Peake et al., 2014; Sato,
324 Cheng, Kawamura, Takae, & Hsueh, 2012; Xi et al., 2019). Beyond the role of CNP
325 as an oocyte meiotic arrest factor, previous studies by our group and others confirmed
326 that adding CNP to the pre-IVM system significantly improved oocyte maturation and
327 subsequent embryo developmental potential (Richani & Gilchrist, 2022; Soto-Heras,
328 Paramio, & Thompson, 2019; Wei et al., 2017). The synchronization of nuclear and
329 cytoplasmic maturation is essential for oocyte quality and supporting early embryonic
330 preimplantation development. However, the underlying molecular mechanism and
331 whether CNP has any beneficial effect on the maternal age-induced decline in oocyte
332 quality are incompletely understood. In the present study, we showed that CNP levels
333 declined with age and demonstrated that CNP supplementation increased the number
334 of antral follicles and the ovulation rate and enhanced oocyte quality and fertility.
335 Furthermore, supplementation of CNP in pre-IVM oocyte culture medium reversed
336 the adverse effects of age on immature oocytes, offering a potentially effective

337 approach for assisted reproductive technologies to acquire a greater number of high-
338 quality oocytes and improve the fertility of older women.

339 Many factors affect the adverse effects on the oocyte maturation process and
340 embryonic development associated with advanced maternal age (Mikwar, MacFarlane,
341 & Marchetti, 2020). Assisted reproductive technologies are an efficient scheme to
342 resolve infertility as maternal fertility declines with ageing. However, the low success
343 rate of IVM oocytes, which is especially pronounced in maternally aged oocytes,
344 limits fertilization outcomes. Our in vivo results showed that CNP supplementation
345 results in multiple improvements, including reductions in oxidative damage, spindle
346 defects, and abnormal organelle distributions and functions, in maternally aged
347 oocytes. Thus, we further investigated the use of CNP in the IVM system, especially
348 in improving the quality of oocytes derived from aged mice. The results indicated that
349 CNP-induced temporary meiotic arrest improved the maturation and fertilization rate
350 of maternally aged oocytes and increased their subsequent embryo developmental
351 competence. Specifically, our results confirmed an advanced role for CNP in
352 preventing the development of mitochondrial structure abnormalities and the typical
353 dysfunctional processes in aged oocytes. Furthermore, these data showed that CNP
354 apparently partially rescued the antioxidant defence system impairment
355 accompanying oocyte ageing and alleviated oxidative stress. In addition, the findings
356 demonstrated that CNP improved cytoplasmic maturation events by maintaining
357 normal CG, ER and Golgi apparatus distribution and function in aged oocytes.

358 The asynchronous nature of nuclear and cytoplasmic maturation is a major
359 challenge in improving the quality of IVM oocytes (Coticchio et al., 2015). Age-
360 related aberrant chromosome alignment prior to cytoplasmic maturation may result in
361 poor oocyte quality and subsequent reduced reproductive potential (Russ, Haywood,
362 Lane, Schoolcraft, & Katz-Jaffe, 2022). In the present study, after COCs were induced,
363 the temporary meiotic arrest resulting from CNP treatment significantly increased the
364 maturation rate, which may synchronize oocyte nuclear and cytoplasmic maturation.
365 Organelle distribution is a necessary feature of oocyte cytoplasmic maturation and
366 subsequent development. Dramatic ER reorganization (FitzHarris, Marangos, &
367 Carroll, 2007), CG translocation to the cell cortex (Liu, Sims, Calarco, & Talbot,
368 2003), and the Golgi apparatus distribution and function are commonly regarded as
369 indicators of cytoplasmic maturation (Mao, Lou, Lou, Wang, & Jin, 2014). Similarly,
370 our results demonstrate that CNP supplementation restored cytoplasmic maturation in
371 maternally aged oocytes by ensuring normal organelle distribution dynamics and
372 organelle function, increasing the fertilization capacity and developmental
373 competence of aged oocytes. It is reasonable to assume that CNP is a potential option
374 to prevent abnormal organelle distribution and functions in oocytes that could be
375 triggered by ubiquitous environmental endocrine disruptors, such as bisphenol A and
376 citrinin (Pan et al., 2021; Sun et al., 2020). Cortical granules (CGs) are oocyte-
377 specific vesicles located under the subcortex. Fusion of CGs with the oocyte plasma
378 membrane is the most important event needed to prevent polyspermy (Miao et al.,

379 2020). The distribution of CGs is usually regarded as one of the most important
380 indicators of oocyte cytoplasmic maturation. The contents of the CGs are normally
381 discharged by exocytosis when the egg is stimulated by the fertilizing spermatozoon;
382 this process is called the cortical reaction, and it prevents polyspermy and protects the
383 embryo from a hostile environment during early development (Schuel, 1978).

384 One of the major known causes of oocyte oxidative damage and apoptosis arises
385 from excessive ROS accumulation with ageing, especially in IVM oocytes
386 (Combelles, Gupta, & Agarwal, 2009; Soto-Heras & Paramio, 2020). Excessive ROS
387 accumulation occurs as a result of two processes, namely, constant generation in the
388 mitochondria or scavenging by antioxidant defence systems, both of which involve
389 age-related quality decreases in oocytes (Mianqun Zhang, Lu, Chen, Zhang, & Xiong,
390 2020). Thus, maintaining the balance between the production and scavenging of ROS
391 could help to alleviate age-related oxidative damage and fertility decreases. Some
392 antioxidative factor(s) within oocytes might deteriorate as the potential mother ages,
393 compromising the ability for ROS scavenging (Schwarzer et al., 2014). GSH serves as
394 one of the antioxidants in oocytes to combat ROS-mediated oxidative stress, which is
395 highly correlated with oocyte developmental competence (Furnus et al., 2008). The
396 present results suggested that CNP-induced temporary meiotic arrest increased the
397 GSH/GSSG ratio, which is involved in the enhancement of oocyte antioxidant
398 defence and may contribute to improving oocyte developmental competence.
399 Consistent with previous studies (Miao et al., 2020), our findings validated that

400 maternal ageing results in excessive accumulation of ROS and DNA damage, which
401 severely impairs follicle development, ovulation, oocyte quality and subsequent
402 embryo developmental potential.

403 Defects in chromosome separation and decondensation as well as chromosomal
404 misalignment caused by spindle detachment are the major contributing factors
405 responsible for the decline in oocyte quality with ageing (Chiang, Schultz, &
406 Lampson, 2011; Eichenlaub-Ritter, Vogt, Yin, & Gosden, 2004). Oocytes require ATP
407 for spindle formation, chromosome segregation, and polar body extrusion and
408 fertilization processes (Arhin, Lu, Xi, & Jin, 2018; Eichenlaub-Ritter, 2013).
409 Mitochondria are the most abundant organelles in oocytes and play an important role
410 in ATP production via oxidative phosphorylation to phosphorylate adenosine
411 diphosphate (Bentov, Yavorska, Esfandiari, Jurisicova, & Casper, 2011). Thus,
412 mitochondrial function is a key indicator of oocyte quality and successful fertilization
413 in assisted reproductive technologies (ARTs) (Mikwar et al., 2020). Mitochondrial
414 metabolic activity and mitochondrial DNA replication dramatically decrease in
415 oocytes with maternal age, which reduces ATP production; leads to meiotic spindle
416 damage, chromosome misalignment and aneuploidy; and largely impairs oocyte
417 maturation processes (Eichenlaub-Ritter, Wieczorek, Lüke, & Seidel, 2011; May-
418 Panloup et al., 2016). We demonstrated that CNP reverses mitochondrial dysfunction
419 induced by ageing in oocytes by analysing the mitochondrial distribution, ATP content,
420 and mitochondrial membrane potential ($\Delta\Psi m$).

421 Notably, disruption of the mitochondrial membrane potential is a potent trigger
422 of mitophagy (Matsuda et al., 2010). Our single-cell transcriptome profiling data
423 showed that the expression of genes related to ubiquitin-mediated proteolysis and the
424 mitophagy pathway was considerably upregulated in aged oocytes but restored to
425 normal levels following CNP supplementation. We also observed by TEM that CNP
426 supplementation suppressed the accumulation of autophagic vesicles containing
427 mitochondria. Furthermore, immunoblot analysis revealed degradation of the
428 autophagy biomarker p62 and accumulation of LC3-II in aged oocytes, events that
429 were markedly suppressed in CNP-treated oocytes. In general, excessive activation of
430 mitophagy and mitochondrial damage in aged oocytes may be involved in the
431 deterioration of oocyte quality, while CNP can ameliorate this process.

432 The PINK1/Parkin pathway is one of the most studied ubiquitin-dependent
433 mitophagy processes and is crucial for the equilibrium between mitochondrial
434 biogenesis and mitochondrial removal via selective recognition and elimination of
435 dysfunctional mitochondria (Ateneo, 2019). In healthy mitochondria, the
436 serine/threonine kinase PINK1 is usually expressed at low levels, but it rapidly
437 accumulates on damaged or aged mitochondria that exhibit loss of membrane
438 potential (Narendra & Youle, 2011). The decrease in the mitochondrial membrane
439 potential abolishes translocation across the outer and inner membranes and confines
440 PINK1 in the mitochondrial matrix, stabilizing it on the mitochondrial outer
441 membrane in a complex with the translocase TOM (De Gaetano et al., 2021).

442 Stabilized PINK1 recruits the cytosolic E3-ubiquitin ligase Parkin from the cytosol to
443 damaged mitochondria, an event followed by mitophagy. The effects of CNP on
444 meiotic arrest depend on the maintenance of cAMP levels in oocytes (Meijia Zhang et
445 al., 2010). Recent findings revealed that cAMP-dependent activation of PKA reduced
446 the PINK1 protein level due to its rapid degradation via the proteasome and severely
447 inhibited Parkin recruitment to depolarized mitochondria (Lobo et al., 2020). Our data
448 confirmed that PINK1 expression was decreased in CNP-treated oocytes, thus leading
449 to a reduction in Parkin recruitment. However, these effects were disrupted by the
450 inhibition of PKA pathway activity, indicating that cAMP indeed mediates the
451 ameliorating effects of CNP on aged oocyte quality. Taken together, these findings
452 indicate that PKA-mediated inhibition of Parkin recruitment may contribute to
453 protecting mitochondria with a low membrane potential from mitophagy in aged
454 oocytes.

455 Collectively, our studies demonstrated that CNP improves the fertilization and
456 developmental competence of maternally aged mouse oocytes by preventing age-
457 related antioxidant defects and excessive mitophagy. Considering its known
458 contributions as a physiological meiotic inhibitor, CNP provides an alternative to
459 prevent maternal age-related oocyte quality defects and improve developmental
460 competence. Although ARTs have been widely used to treat infertility, their overall
461 success rates in women of advanced maternal age remain low. Our data may provide a
462 new theoretical basis for the use of CNP in improving subfertility in older women or

463 the application of clinically assisted reproduction. Out of caution, however,
464 randomized controlled clinical trials should be conducted to further study the efficacy
465 of CNP in women who wish to become pregnant.

466 **MATERIALS AND METHODS**

467 **Animals and ethics statement**

468 The young (6~8-week-old) and aged (58~60-week-old) C57BL-6J female mice
469 were obtained from the Experimental Animal Center of the Xi'an Jiaotong University
470 and housed in a temperature (20~25℃) and light-controlled environment (12 h light–
471 12 h dark cycle) and provided with food and water ad libitum. All the experimental
472 protocols and mice handling procedures were reviewed and approved by the
473 Institutional Animal Care and Use Committee of the College of Veterinary Medicine,
474 Northwest A&F University (No. 2018011212).

475 **In vivo treatment with CNP**

476 Aged mice (58-week-old) were intraperitoneally injected daily with CNP (120
477 μg/kg body weight; Cat#B5441, ApexBio) for 14 days. CNP was dissolved in PBS
478 and diluted to appropriate concentration by physiological saline solution before
479 injection. The mice were followed by a single injection of 5 IU pregnant mare serum
480 gonadotropin (PMSG; Ningbo Second Hormone Factory, Ningbo, China) for 46 h to
481 stimulate penultimate follicle maturation before collection of ovaries for histological
482 analyses and weighting. Some mice were further injected with 5 IU human chorionic
483 gonadotropin (hCG; Ningbo Second Hormone Factory, Ningbo, China), and the

484 ovulated oocytes in oviducts were monitored 16 h later to evaluate ovulation
485 efficiency.

486 **Measurement of CNP levels**

487 CNP was measured in plasma by a two-site polyclonal direct ELISA kit
488 (Biomedica Medizinprodukte, Vienna, Austria) according to the manufacturer's
489 instructions. Collect blood samples in standardized serum separator tubes (SST),
490 allow samples to clot for 30 minutes at room temperature and perform serum
491 separation by centrifugation. Assay the acquired serum samples immediately. Read
492 the optical density (OD) of all wells on a plate reader using 450 nm wavelength.
493 Construct a standard curve from the absorbance read-outs of the standards. Obtain
494 sample concentrations from the standard curve.

495 **Histological analysis of ovaries**

496 Ovaries from each group of mice were fixed in 4% paraformaldehyde (pH 7.5)
497 overnight at 4℃, dehydrated using graded ethanol, followed by xylenes and
498 embedded in paraffin. Paraffin-embedded ovaries were serial sectioned at a thickness
499 of 5 μm for hematoxylin and eosin (H&E) staining. Ovaries from three mice of each
500 group were used for the analysis.

501 **Collection and culture of cumulus-oocyte complexes (COCs)**

502 Female mice were stimulated by an intraperitoneal injection of 5 IU PMSG, and
503 mice were sacrificed by cervical dislocation 24 h later. The ovaries were collected,

504 and the well-developed Graafian follicles were punctured with 30-gauge needles to
505 collect COCs. Only COCs with morphological integrity and a distinct germinal
506 vesicle (GV) were cultured in basic culture medium consisted of Minimum Essential
507 Medium (MEM)-α (Life Technologies, New York, USA) supplemented with 3mg/mL
508 bovine serum albumin and 0.23 mM pyruvate at 37°C under an atmosphere of 5%
509 CO_2 in air with maximum humidity.

510 **CNP treatment and in vitro maturation**

511 For in vitro induce temporary meiotic arrest, COCs were cultured in basic culture
512 medium containing 10 nM of CNP. The dose of CNP for meiotic arrest in mouse
513 oocytes in vitro was selected based on the published literatures (Meijia Zhang et al.,
514 2011) and our preliminary reports (Wei et al., 2017). After meiotic arrest culture for
515 24 h, COCs were transferred to CNP-free IVM medium (containing 10 ng/mL
516 epidermal growth factor (EGF)) to induce maturation. After incubation for 16 h,
517 COCs were denuded of cumulus cells by treatment with 0.03% hyaluronidase to
518 obtain MII oocytes for future experiments.

519 **In vitro fertilization and embryo culture**

520 Caudae epididymides from 12-week-old male C57BL-6J mice were lanced in a
521 dish of in human tubal fluid (HTF) medium to release sperm, followed by being
522 capacitated for 1 h (37°C under an atmosphere of 5% CO_2 in air with maximum
523 humidity). Maturated oocytes were incubated with capacitated sperm at a

524 concentration of 4×10^5/mL in 100 μL HTF for 6 h at 37°C, 5% CO_2. The presence of
525 two pronuclei was scored as successful fertilization. The embryos were cultured in
526 KSOM under mineral oil at 37 °C in 5% CO_2 and saturated humidity.

527 **Preantral follicle isolation and culture**

528 Ovaries were removed after the animals had been killed by cervical dislocation
529 and preantral follicles were mechanically isolated using 26-gauge needles. Then, the
530 preantral follicles (80–100μm diameter) that enclosed by an intact basal membrane
531 were collected, distributed randomly and cultured individually in 96-well tissue
532 culture plates for up to 6 days at 37°C in a humidified atmosphere of 5% CO_2 in air.
533 The basic culture medium consisted of MEM-α supplemented with 1mg/mL BSA, 1%
534 ITS (5μg/ mL insulin, 5μg/mL transferrin, 5ng/mL selenium; Sigma), 100μg/mL
535 sodium pyruvate and 1% penicillin/streptomycin sulfate (Sigma) in the absence
536 (control) or presence of 100nM CNP or 10 μM H89. The dose of CNP was selected
537 based on the published literatures (Xi et al., 2019). Half the medium was replaced
538 with fresh medium and follicles were photographed every other day, and follicle
539 diameter was measured using ImageJ at each time point.

540 **Immunofluorescent Staining**

541 Oocytes were fixed in 4% paraformaldehyde in PBS for 30 min at room
542 temperature, and permeabilized with 0.5% Triton X-100 for 20 min, then blocked
543 with 1% BSA in PBS for 1 h at room temperature. The oocytes were incubated with

544 primary antibodies (Alexa Fluor® 488 Conjugate anti-α-tubulin monoclonal
545 antibody,1:200, Cell Signaling, Cat#35652; rabbit anti-Tom20 antibody, 1:100, Cell
546 Signaling, Cat#sc-42406; mouse anti-Parkin antibody, 1:100, Santa Cruz, Cat#sc-
547 32282) at 4°C overnight, and then the oocytes were extensively washed with wash
548 buffer (0.1% Tween 20 in PBS), probed with Alexa Fluor 488 goat anti-rabbit IgG
549 (1:200, Thermo Fisher Scientific, A21206) or Alexa Fluor 594 donkey anti-mouse
550 IgG (1:200, Abcam, ab150108) in a dark room for 1 h at room temperature. Then
551 oocytes were counterstained with DAPI (10 μg/mL) at room temperature for 10 min.
552 Finally, samples were mounted on glass slides and observed viewed under the
553 confocal microscope (Nikon A1R-si).

554 **Mito-Tracker, ER-Tracker, and Golgi-Tracker Red Staining**

555 Oocytes were incubated with Mito-tracker Red (1:2000, Beyotime
556 Biotechnology, Shanghai, China), ER-Tracker Red (1:3000, Beyotime Biotechnology),
557 Golgi-Tracker Red (1:50, Beyotime Biotechnology) in M2 medium for 30 min at
558 37 °C in a 5% CO_2 and saturated humidity. Then, the oocytes were counterstained
559 with DAPI (10 μg/mL) for 5min at 37 °C in a 5% CO_2 and saturated humidity, and
560 finally, the samples were washed 3 times with M2 medium and examined with a
561 confocal laser-scanning microscope (Nikon A1R-si).

562 **Mitochondrial membrane potential (ΔΨm) measurement**

563 Oocyte mitochondrial membrane potential was evaluated using Mito-Probe JC-1

564 Assay Kit (Beyotime Institute of Biotechnology, Shanghai, China). Briefly, oocytes
565 were incubated with 2 μM JC-1 in M2 medium for 30 min at 37 °C in a 5% CO_2 and
566 saturated humidity, and finally, the samples were washed 3 times with M2 medium
567 and examined with a confocal laser-scanning microscope (Nikon A1R-si). JC-1 dye
568 exhibits a fluorescence emission of green (529 nm) and red (590 nm). Thus, the
569 red/green fluorescence intensity ratio was measured to indicate mitochondrial
570 depolarization. Oocytes mitochondrial membrane potential (ΔΨm) measurements
571 were performed as our previous report (H. Zhang et al., 2020).

572 **Monitoring of ROS levels in oocytes**

573 The amount of ROS in oocytes was processed with 10 μM oxidation sensitive
574 fluorescent probe dichlorofluorescein (DCFH) (Beyotime Institute of Biotechnology,
575 Shanghai, China) for 30 min at 37°C in M2 medium. Then oocytes were washed three
576 times with M2 medium and placed on glass slides for image capture under a confocal
577 microscope (Nikon A1R-si).

578 Determination of mitochondrial ROS (mitoSOX) generation by MitoSOX
579 staining, GV oocytes were incubated in M2 media containing 5 μM MitoSOX Red
580 (ThermoFisher, M36008, Waltham, USA,) in humidified atmosphere for 10 min at
581 37°C. After washing three times in M2 media, oocytes were imaged under a confocal
582 microscope (Nikon A1R-si).

583 **Measurement of the GSH/GSSG ratio**

584 The GSH/GSSG ratio was measured with a GSSG/GSH Assay Kit (Beyotime
585 Institute of Biotechnology) according to the manufacturer's instructions. Briefly,
586 oocytes were lysed in 40 μL deproteinized buffer on ice for 10 min. The lysate was
587 centrifuged at 12000×g for 5 min at 4 °C. For GSSG measurement, the samples were
588 incubated with GSH scavenge buffer for 60 min at 25 °C to decompose GSH. Then,
589 the samples were transferred to the 96-well plates and the absorbance was measured
590 with a multimode plate reader (BioTek Epoch) at 412 nm.

591 **Measurement of the oocyte NADPH content**

592 The oocyte NADPH contents were measured using a NADPH assay kit
593 (Beyotime Institute of Biotechnology) according to the manufacturer's instructions.
594 Briefly, 50 ~ 60 oocytes per group were lysed in 100 μL NADPH extraction buffer on
595 ice for 20 min. After the samples were centrifuged at 12000×*g* for 5 min at 4 °C, the
596 supernatants were transferred to the 96-well plates (50μl per well), and the absorbance
597 was measured using a multimode plate reader (BioTek Epoch) at 450 nm. The amount
598 of NADPH was determined using a calibration curve.

599 **Western blot analysis**

600 Approximately 200 oocytes were lysed in RIPA buffer (solarbio, Beijing, China)
601 that supplemented with 1mM protease inhibitors phenylmethylsulfonyl fluoride
602 (PMSF, solarbio, Beijing, China), on ice for 30 min. Samples were boiled at 100 °C in
603 a metal bath for 10 min in protein loading buffer (CoWin Biosciences, Beijing, China)

604 and equal amount proteins were separated by 10% SDS-PAGE gel, and transferred to
605 polyvinylidene fluoride (PVDF) membranes (Millipore, Bedford, USA). After transfer,
606 the membranes were blocked in TBST that contained 3 % BSA for 1 h at room
607 temperature, followed by incubation with primary antibodies at 4 °C overnight (the
608 primary antibodies were rabbit anti-GAPDH antibody, 1:2000, Cell Signaling,
609 Cat#5174; rabbit anti-p62 antibody, 1:1000, Cell Signaling, Cat#23214; rabbit anti-
610 Tom20 antibody, 1:1000, Cell Signaling, Cat#sc-42406; rabbit anti-LC3A/B antibody,
611 1:1000, Abcam, Cat#ab128025; rabbit anti-PINK1 antibody, 1:1000, Cell Signaling,
612 Cat#6946; mouse anti-Parkin antibody, 1:1000, Santa Cruz, Cat#sc-32282). The
613 secondary antibodies were incubated for 1 h at room temperature, and then the
614 membrane signals were visualized by a chemiluminescent HRP substrate reagent
615 (Bio-rad Laboratories, Hercules, CA, USA) and images were captured with
616 Tanon5200 Imaging System (Biotanon, Shanghai, China). The band intensity was
617 assessed with Image J software and normalized to that of GAPDH.

618 **Transmission electron microscope (TEM)**

619 Oocytes were prefixed with 3% glutaraldehyde, refixed with 1% osmium
620 tetroxide, dehydrated in acetone, and embedded in Ep812 (Can EM Ltd.). Semithin
621 sections were stained with toluidine blue for optical positioning, and ultrathin sections
622 were made with a diamond knife and observed by a JEM-1400FLASH transmission
623 electron microscope (JEOL) after staining with uranyl acetate and lead citrate.

624 **Evaluation of total ATP content**

625 The ATP content of oocytes was detected with an ATP Bioluminescence Assay
626 Kit (Beyotime Institute of Biotechnology). The oocytes were lysed with 50 μl of ATP
627 lysis buffer on ice, centrifuged at 12000 × g at 4°C for 5 minutes, and the supernatants
628 were transferred to a 96-well black culture plate. Then, the samples and standards
629 were read with a Multimode Microplate Reader (Tecan Life Sciences). Finally, the
630 ATP level was calculated according to the standard curve.

631 **RNA sequencing and analysis**

632 GV-stage oocytes were collected from three young, three aged and three CNP
633 treated aged mice. mRNA samples were collected from 5 oocytes from the same
634 mouse of each group. The mRNA was directly reverse-transcribed through oligo dT.
635 The reverse-transcribed cDNA was amplified, and the cDNA was cut by Tn5
636 transposase digestion, and linkers were added to obtain the required sequencing
637 library. The constructed library was entered into the sequencing program after passing
638 through an Agilent 2100 Bioanalyzer and RT–PCR quality control. The PE100
639 sequencing strategy was used to assess gene expression changes at the transcription
640 level. Dr. Tom was used for difference analysis, GO analysis, KEGG analysis, and
641 other analyses.

642 **Reverse transcriptase quantitative PCR (RT-qPCR) analysis**

643 Total RNA from oocytes was extracted using MiniBEST Universal RNA

644 Extraction Kit (TaKaRa, Dalian, China), and reverse transcribed to synthesize cDNA
645 using a PrimeScript RT Master Mix reverse transcription kit (TaKaRa) according to
646 the manufacturer's instructions. RT-qPCR quantitation of mRNAs was performed
647 using TB Green™ Premix Ex Taq™ II (TaKaRa) with Applied Biosystems
648 StepOnePlus Real-Time PCR System (Thermo Fisher Scientific, Massachusetts, USA)
649 using the following parameters: 95 °C for 1 min, followed by 40 cycles at 95 °C for 5
650 s and 60 °C for 34 s. The PCR primers used in this study were shown in Table S1.
651 Transcript levels were normalized to those of the housekeeping gene *Gapdh*. The CT
652 value was used to calculate the fold change using the $2^{-\triangle\triangle Ct}$ method. Each experiment
653 was repeated independently at least thrice.

654 **Statistical analysis**

655 Statistical analyses were performed using GraphPad Prism 8.00 software
656 (GraphPad, CA, United States). Data were reported as means ± SEM. Results of
657 statistically significant differences were denoted by asterisk. ($P < 0.05$ denoted by *, P
658 < 0.01 denoted by **, $P < 0.001$ denoted by ***, and $P < 0.0001$ denoted by ****).

659 **Ethics approval**

660 The experimental protocols and mice handling procedures were reviewed and
661 approved by the Institutional Animal Care and Use Committee of the College of
662 Veterinary Medicine, Northwest A&F University (No. 2018011212).

663 **Conflicts of interest**

664 All of the contributing authors declared no conflicts of interest. All authors read

and approved the final manuscript.

Data availability statement

All data is included in the manuscript and supporting information.

Acknowledgments

We thank other members in the Ma laboratory for their helpful discussion on the manuscript. This work was supported in part by National Natural Science Foundation of China (31772818).

References

Adhikari, D., Lee, I.-w., Yuen, W. S., & Carroll, J. (2022). Oocyte mitochondria—key regulators of oocyte function and potential therapeutic targets for improving fertility. *Biology of Reproduction, 106*(2), 366-377.

Akabane, S., Uno, M., Tani, N., Shimazaki, S., Ebara, N., Kato, H., . . . Oka, T. (2016). PKA regulates PINK1 stability and Parkin recruitment to damaged mitochondria through phosphorylation of MIC60. *Molecular cell, 62*(3), 371-384.

Amer, Y. O., & Hebert-Chatelain, E. (2018). Mitochondrial cAMP-PKA signaling: What do we really know? *Biochimica et Biophysica Acta (BBA)-Bioenergetics, 1859*(9), 868-877.

Arhin, S. K., Lu, J., Xi, H., & Jin, X. (2018). Energy requirements in mammalian oogenesis. *Cellular and Molecular Biology, 64*(10), 12-19.

Ateneo, F. S. (2019). Mitophagy and Oxidative Stress in Cancer and Aging: Focus on Sirtuins and Nanomaterials. *Journal: Oxidative Medicine and Cellular Longevity*, 1-19.

Bae, C.-R., Hino, J., Hosoda, H., Arai, Y., Son, C., Makino, H., . . . Nojiri, T. (2017). Overexpression of C-type natriuretic peptide in endothelial cells protects against insulin resistance and inflammation during diet-induced obesity. *Scientific reports, 7*(1), 1-13.

Bartimaeus, E.-A. S., Obi, C. E., Igwe, F. U., & Nwachuku, E. O. (2020). Impact of Age on Hormonal Profiles of Sub-Fertile Women Attending Fertility Clinic in Umuahia, Abia State, South Eastern Nigeria. *Open Journal of Internal Medicine, 10*(01), 51.

Bentov, Y., Yavorska, T., Esfandiari, N., Jurisicova, A., & Casper, R. F. (2011). The

contribution of mitochondrial function to reproductive aging. *Journal of assisted reproduction and genetics, 28*(9), 773-783.

Broekmans, F., Soules, M., & Fauser, B. (2009). Ovarian aging: mechanisms and clinical consequences. *Endocrine reviews, 30*(5), 465-493.

Chang, E. M., Song, H. S., Lee, D. R., Lee, W. S., & Yoon, T. K. (2014). In vitro maturation of human oocytes: its role in infertility treatment and new possibilities. *Clinical and experimental reproductive medicine, 41*(2), 41.

Chiang, T., Schultz, R. M., & Lampson, M. A. (2011). Age-dependent susceptibility of chromosome cohesion to premature separase activation in mouse oocytes. *Biology of reproduction, 85*(6), 1279-1283.

Combelles, C. M., Gupta, S., & Agarwal, A. (2009). Could oxidative stress influence the in-vitro maturation of oocytes? *Reproductive biomedicine online, 18*(6), 864-880.

Coticchio, G., Dal Canto, M., Mignini Renzini, M., Guglielmo, M. C., Brambillasca, F., Turchi, D., . . . Fadini, R. (2015). Oocyte maturation: gamete-somatic cells interactions, meiotic resumption, cytoskeletal dynamics and cytoplasmic reorganization. *Human Reproduction Update, 21*(4), 427-454.

De Gaetano, A., Gibellini, L., Zanini, G., Nasi, M., Cossarizza, A., & Pinti, M. (2021). Mitophagy and oxidative stress: The role of aging. *Antioxidants, 10*(5), 794.

Eichenlaub-Ritter, U. (2013). Oocyte ageing and its cellular basis. *International Journal of Developmental Biology, 56*(10-11-12), 841-852.

Eichenlaub-Ritter, U., Vogt, E., Yin, H., & Gosden, R. (2004). Spindles, mitochondria and redox potential in ageing oocytes. *Reproductive biomedicine online, 8*(1), 45-58.

Eichenlaub-Ritter, U., Wieczorek, M., Lüke, S., & Seidel, T. (2011). Age related changes in mitochondrial function and new approaches to study redox regulation in mammalian oocytes in response to age or maturation conditions. *Mitochondrion, 11*(5), 783-796.

FitzHarris, G., Marangos, P., & Carroll, J. (2007). Changes in endoplasmic reticulum structure during mouse oocyte maturation are controlled by the cytoskeleton and cytoplasmic dynein. *Developmental biology, 305*(1), 133-144.

Furnus, C. C., De Matos, D., Picco, S., García, P. P., Inda, A. M., Mattioli, G., & Errecalde, A. L. (2008). Metabolic requirements associated with GSH synthesis during in vitro maturation of cattle oocytes. *Animal reproduction science, 109*(1-4), 88-99.

Gandolfi, T. B., & Gandolfi, F. (2001). The maternal legacy to the embryo: cytoplasmic components and their effects on early development. *Theriogenology, 55*(6), 1255-1276.

Jiang, Y., Shen, M., Chen, Y., Wei, Y., Tao, J., & Liu, H. (2021). Melatonin represses mitophagy to protect mouse granulosa cells from oxidative damage.

Biomolecules, 11(7), 968.

Jin, X., Wang, K., Wang, L., Liu, W., Zhang, C., Qiu, Y., . . . Yang, Z. (2022). RAB7 activity is required for the regulation of mitophagy in oocyte meiosis and oocyte quality control during ovarian aging. *Autophagy, 18*(3), 643-660.

Liu, M., Sims, D., Calarco, P., & Talbot, P. (2003). Biochemical heterogeneity, migration, and pre-fertilization release of mouse oocyte cortical granules. *Reproductive Biology and Endocrinology, 1*(1), 1-11.

Lobo, M. J., Reverte-Salisa, L., Chao, Y.-C., Koschinski, A., Gesellchen, F., Subramaniam, G., . . . Paolocci, E. (2020). Phosphodiesterase 2A2 regulates mitochondria clearance through Parkin-dependent mitophagy. *Communications biology, 3*(1), 1-16.

Ma, J.-Y., Li, S., Chen, L.-N., Schatten, H., Ou, X.-H., & Sun, Q.-Y. (2020). Why is oocyte aneuploidy increased with maternal aging? *Journal of genetics and genomics, 47*(11), 659-671.

Mao, L., Lou, H., Lou, Y., Wang, N., & Jin, F. (2014). Behaviour of cytoplasmic organelles and cytoskeleton during oocyte maturation. *Reproductive biomedicine online, 28*(3), 284-299.

Matsuda, N., Sato, S., Shiba, K., Okatsu, K., Saisho, K., Gautier, C. A., . . . Sato, F. (2010). PINK1 stabilized by mitochondrial depolarization recruits Parkin to damaged mitochondria and activates latent Parkin for mitophagy. *Journal of Cell Biology, 189*(2), 211-221.

May-Panloup, P., Boucret, L., Chao de la Barca, J.-M., Desquiret-Dumas, V., Ferré-L'Hotellier, V., Morinière, C., . . . Reynier, P. (2016). Ovarian ageing: the role of mitochondria in oocytes and follicles. *Human Reproduction Update, 22*(6), 725-743.

McClatchie, T., Meredith, M., Ouédraogo, M. O., Slow, S., Lever, M., Mann, M. R., . . . Baltz, J. M. (2017). Betaine is accumulated via transient choline dehydrogenase activation during mouse oocyte meiotic maturation. *Journal of Biological Chemistry, 292*(33), 13784-13794.

Miao, Y., Cui, Z., Gao, Q., Rui, R., & Xiong, B. (2020). Nicotinamide mononucleotide supplementation reverses the declining quality of maternally aged oocytes. *Cell reports, 32*(5), 107987.

Mikwar, M., MacFarlane, A. J., & Marchetti, F. (2020). Mechanisms of oocyte aneuploidy associated with advanced maternal age. *Mutation Research/Reviews in Mutation Research*, 108320.

Miyazaki, S., & Ito, M. (2006). Calcium signals for egg activation in mammals. *Journal of pharmacological sciences, 100*(5), 545-552.

Moyes, A. J., & Hobbs, A. J. (2019). C-type natriuretic peptide: a multifaceted paracrine regulator in the heart and vasculature. *International journal of molecular sciences, 20*(9), 2281.

Narendra, D. P., & Youle, R. J. (2011). Targeting mitochondrial dysfunction: role for PINK1 and Parkin in mitochondrial quality control. *Antioxidants & redox signaling, 14*(10), 1929-1938.

Pan, M.-H., Wu, Y.-K., Liao, B.-Y., Zhang, H., Li, C., Wang, J.-L., . . . Ma, B. (2021). Bisphenol A Exposure Disrupts Organelle Distribution and Functions During Mouse Oocyte Maturation. *Frontiers in Cell and Developmental Biology, 9*, 656.

Peake, N., Hobbs, A., Pingguan-Murphy, B., Salter, D., Berenbaum, F., & Chowdhury, T. (2014). Role of C-type natriuretic peptide signalling in maintaining cartilage and bone function. *Osteoarthritis and cartilage, 22*(11), 1800-1807.

Reader, K. L., Stanton, J.-A. L., & Juengel, J. L. (2017). The role of oocyte organelles in determining developmental competence. *Biology, 6*(3), 35.

Richani, D., & Gilchrist, R. B. (2022). Approaches to oocyte meiotic arrest in vitro and impact on oocyte developmental competence. *Biology of Reproduction, 106*(2), 243-252.

Russ, J. E., Haywood, M. E., Lane, S. L., Schoolcraft, W. B., & Katz-Jaffe, M. G. (2022). Spatially resolved transcriptomic profiling of ovarian aging in mice. *Iscience, 25*(8), 104819.

Sato, Y., Cheng, Y., Kawamura, K., Takae, S., & Hsueh, A. J. (2012). C-type natriuretic peptide stimulates ovarian follicle development. *Molecular endocrinology, 26*(7), 1158-1166.

Schuel, H. (1978). Secretory functions of egg cortical granules in fertilization and development: A critical review. *Gamete Research, 1*(3‐4), 299-382.

Schwarzer, C., Siatkowski, M., Pfeiffer, M. J., Baeumer, N., Drexler, H., Wang, B., . . . Boiani, M. (2014). Maternal age effect on mouse oocytes: new biological insight from proteomic analysis. *Reproduction, 148*(1), 55-72.

Shen, M., Jiang, Y., Guan, Z., Cao, Y., Sun, S.-c., & Liu, H. (2016). FSH protects mouse granulosa cells from oxidative damage by repressing mitophagy. *Scientific reports, 6*(1), 1-13.

Shen, Q., Liu, Y., Li, H., & Zhang, L. (2021). Effect of mitophagy in oocytes and granulosa cells on oocyte quality. *Biology of Reproduction, 104*(2), 294-304.

Soto-Heras, S., & Paramio, M.-T. (2020). Impact of oxidative stress on oocyte competence for in vitro embryo production programs. *Research in Veterinary Science*.

Soto-Heras, S., Paramio, M.-T., & Thompson, J. G. (2019). Effect of pre-maturation with C-type natriuretic peptide and 3-isobutyl-1-methylxanthine on cumulus-oocyte communication and oocyte developmental competence in cattle. *Animal reproduction science, 202*, 49-57.

Sun, M.-H., Li, X.-H., Xu, Y., Xu, Y., Pan, Z.-N., & Sun, S.-C. (2020). Citrinin

exposure disrupts organelle distribution and functions in mouse oocytes. *Environmental research, 185*, 109476.

Watson, A. (2007). Oocyte cytoplasmic maturation: a key mediator of oocyte and embryo developmental competence. *Journal of animal science, 85*(suppl_13), E1-E3.

Wei, Q., Zhou, C., Yuan, M., Miao, Y., Zhao, X., & Ma, B. (2017). Effect of C-type natriuretic peptide on maturation and developmental competence of immature mouse oocytes in vitro. *Reproduction, Fertility and Development, 29*(2), 319-324.

Xi, G., Wang, W., Fazlani, S. A., Yao, F., Yang, M., Hao, J., . . . Tian, J. (2019). C-type natriuretic peptide enhances mouse preantral follicle growth. *Reproduction, 157*(5), 445-455.

Zarkovic, N. (2020). Roles and Functions of ROS and RNS in Cellular Physiology and Pathology. In (Vol. 9, pp. 767): MDPI.

Zhang, H., Lu, S., Xu, R., Tang, Y., Liu, J., Li, C., . . . Wei, Q. (2020). Mechanisms of estradiol-induced EGF-like factor expression and oocyte maturation via G protein-coupled estrogen receptor. *Endocrinology, 161*(12), bqaa190.

Zhang, M., Lu, Y., Chen, Y., Zhang, Y., & Xiong, B. (2020). Insufficiency of melatonin in follicular fluid is a reversible cause for advanced maternal age-related aneuploidy in oocytes. *Redox biology, 28*, 101327.

Zhang, M., Su, Y.-Q., Sugiura, K., Wigglesworth, K., Xia, G., & Eppig, J. J. (2011). Estradiol promotes and maintains cumulus cell expression of natriuretic peptide receptor 2 (NPR2) and meiotic arrest in mouse oocytes in vitro. *Endocrinology, 152*(11), 4377-4385.

Zhang, M., Su, Y.-Q., Sugiura, K., Xia, G., & Eppig, J. J. (2010). Granulosa cell ligand NPPC and its receptor NPR2 maintain meiotic arrest in mouse oocytes. *Science, 330*(6002), 366-369.

Zhang, T., Xi, Q., Wang, D., Li, J., Wang, M., Li, D., . . . Jin, L. (2019). Mitochondrial dysfunction and endoplasmic reticulum stress involved in oocyte aging: an analysis using single-cell RNA-sequencing of mouse oocytes. *Journal of ovarian research, 12*(1), 1-9.

Zhenwei, J., & Xianhua, Z. (2019). Pre-IVM treatment with C-type natriuretic peptide in the presence of cysteamine enhances bovine oocytes antioxidant defense ability and developmental competence in vitro. *Iranian journal of veterinary research, 20*(3), 173.

855 **Figure legends**

856 **Figure1. Effects of CNP supplementation on the oocyte quality and female**
857 **fertility in aged mice.** (A) A timeline diagram of CNP administration and
858 superovulation. (B) Representative images of young, aged and CNP administration
859 aged (Aged + CNP) mice as well as their ovaries. (C) Body weights of young, aged
860 and aged + CNP aged mice. (D) Ovarian weights of young, aged and aged + CNP
861 mice. (E) Ratios of ovarian weight to body weight for each group of mice. (F) Serum
862 CNP concentrations were measured in young, aged, and aged + CNP mice. (G)
863 Representative images of the oocyte polar body extrusion in young, aged, and aged +
864 CNP mice. Scale bar: 100 μm. (H) Ovulated oocytes were counted in young, aged,
865 and aged + CNP mice. (I) Rate of polar body extrusion in young, aged, and aged +
866 CNP mice. (J) The rate of fragmented oocytes was recorded in young, aged, and aged
867 + CNP mice. (K) Representative images of ovarian sections from young, aged, and
868 aged+CNP mice. Scale bars: 100 μm. (L) Follicles at different developmental stages
869 were counted in young, aged, and aged+CNP ovaries. (M) Average litter size of mated
870 mice was assessed by mating with two-months old male mice.

871

872 **Figure2. CNP supplementation recovers cytoplasmic maturation events of**
873 **maternally aged mouse oocytes.** (A) Representative images of the spindle
874 morphology and chromosome alignment at metaphase II in young, aged, and aged +
875 CNP mice. Scale bar, 10 μm. (B) The rate of aberrant spindles at metaphase II was
876 recorded in young, aged, and aged + CNP mice. (C) Representative images of the
877 Golgi apparatus distribution at metaphase II in young, aged, and aged + CNP mice.
878 Scale bar, 10 μm. (D) The rate of aberrant Golgi apparatus distribution was recorded
879 in young, aged, and aged + CNP mice. (E) Representative images of the endoplasmic
880 reticulum distribution at metaphase II in young, aged, and aged + CNP mice. Scale
881 bar, 10 μm. (F) The rate of aberrant endoplasmic reticulum distribution was recorded
882 in young, aged, and aged + CNP mice. (G) Representative images of the cortical
883 granules (CGs) distribution in young, aged, and aged + CNP mice. Scale bar, 10 μm.
884 (H) The rate of mislocalized CGs was recorded in the young, aged, and aged + CNP
885 mice. (I) The fluorescence intensity of CG signals was measured in the young, aged,
886 and aged + CNP mice oocyte. (J) Representative images of mitochondrial distribution
887 in the young, aged, and aged + CNP mice oocytes stained with MitoTracker Red.
888 Scale bar, 10 μm. (K) The abnormal rate of mitochondrial distribution was recorded in

889 the young, aged, and aged + CNP mice oocytes. (L) ATP levels were measured in the
890 young, aged, and aged + CNP mice. (M) Mitochondrial membrane potential (ΔΨm)
891 was detected by JC-1 staining in in the young, aged, and aged + CNP mice oocytes.
892 Scale bar, 10 μm. (N) The ratio of red to green fluorescence intensity was calculated
893 in the young, aged, and aged + CNP mice oocytes.
894
895 **Figure 3. Effects of CNP on the ROS content, DNA damage, and apoptosis in**
896 **aged oocytes.** (A) Representative images of ROS levels detected by DCFH staining in
897 the young, aged, and aged + CNP mice oocytes. Scale bar, 100 μm. (B) The
898 fluorescence intensity of ROS signals was measured in the young, aged, and aged +
899 CNP mice oocytes. (C) Oocyte NADPH levels in the young, aged, and aged + CNP
900 mice were measured. (D) The ratio of GSH/GSSG was measured in the young, aged,
901 and aged + CNP mice oocytes. (E) Representative images of DNA damage stained
902 with the γ-H2AX antibody in young, aged, and aged + CNP oocytes. Scale bar, 10 μm.
903 (F) γ-H2AX fluorescence intensity was counted in young, aged, and aged + CNP
904 oocytes. (G) Representative images of apoptotic status, assessed by Annexin-V
905 staining, in young, aged, and aged + CNP oocytes. Scale bar, 20 μm. (H) The
906 fluorescence intensity of Annexin-V signals was measured in young, aged, and aged +
907 CNP oocytes.
908
909 **Figure 4. Effects of CNP on the fertilization ability and embryonic development**
910 **of aged oocytes.** (A) Representative images of early embryos developed from young,
911 aged, and aged + CNP oocytes in vitro fertilization. Scale bar, 100 μm. (B) The
912 fertilization rate (2 cell embryos rate), (C) 4 cell embryos rate, (D) 8 cell embryos rate,
913 (E) morula rate and (F) blastocyst formation rates were recorded in the young, aged,
914 and aged + CNP groups. Data in (B)–(F) are presented as mean percentage (mean ±
915 SEM) of at least three independent experiments.
916
917 **Figure 5. Effect of CNP supplementation on transcriptome profiling of aged**
918 **oocytes**
919 (A) Heatmap illustration displaying gene expression of young, aged, and aged+ CNP
920 oocytes. (B) Volcano plot showing differentially expressed genes (DEGs;
921 downregulated, blue; upregulated, red) in Young vs Aged oocytes. Some highly DEGs
922 are listed. (C) Volcano plot showing DEGs in Aged vs Aged + CNP oocytes. Some

923 highly DEGs are listed. (D) KEGG enrichment analysis of upregulated and
924 downregulated DEGs in Young vs Aged oocytes. (E) KEGG enrichment analysis of
925 upregulated and downregulated DEGs in Aged vs Aged + CNP oocytes.
926
927 **Figure 6. Evaluation of CNP supplementation on mitophagy activity of aged**
928 **oocytes.** (A) Representative images of mitochondria morphology and structure in
929 young, aged, and aged + CNP oocytes by TEM. (B) Accumulation of mitochondria
930 damage in young, aged, and aged + CNP oocytes. Under TEM images, percentages of
931 damaged mitochondria per area (500 nm × 500 nm) were shown. At least 4 visions
932 were chosen and mitochondria were counted by two individuals. (C) Representative
933 images of mitochondria ROS stained with MitoSOX in young, aged, aged + CNP
934 oocytes. Scale bar, 20 μm. (D) Fluorescence intensity of MitoSOX signals was
935 measured in young aged, aged + CNP oocytes. (E) Western blots of P62, LC3-I/II,
936 PINK1 and Parkin in young, aged, and aged + CNP oocytes. GAPDH was used as
937 internal control. (F-I) Relative gray value of proteins detected with western blots as
938 compared with controls. (J) Oocyte cAMP concentrations were measured in young,
939 aged, and aged + CNP mice. (K) Representative images at day 0, day 2, day 4 and day
940 6 of cultured preantral follicles with or without CNP or CNP+H89 treatment. Scale
941 bar=50μm. (L) Diameters of preantral follicles with or without CNP or CNP+H89
942 treatment from day 0 to day 6. Six independent culture experiments were performed.
943 (M) Western blots of PINK1 and Parkin in aged, aged + CNP and aged + CNP+H89
944 treated oocytes. GAPDH was used as internal control. (N-O) Relative gray value of
945 proteins detected with western blots as compared with controls. (P) Double
946 immunofluorescence staining of Parkin and TOMM20. The mitochondria outer
947 membrane protein TOMM20 was performed to reveal the translocation of PRKN
948 proteins on mitochondria. Red, PRKN; Green, TOMM20; Blue, DNA was labeled
949 with Hoechst 33342. Bar: 20 μm. (Q) The colocalization of Parkin and TOMM20 in
950 oocytes from aged, aged + CNP and aged + CNP+H89 treated mice were compared.
951 Pearson,s R shows the results of co-location analysis.
952

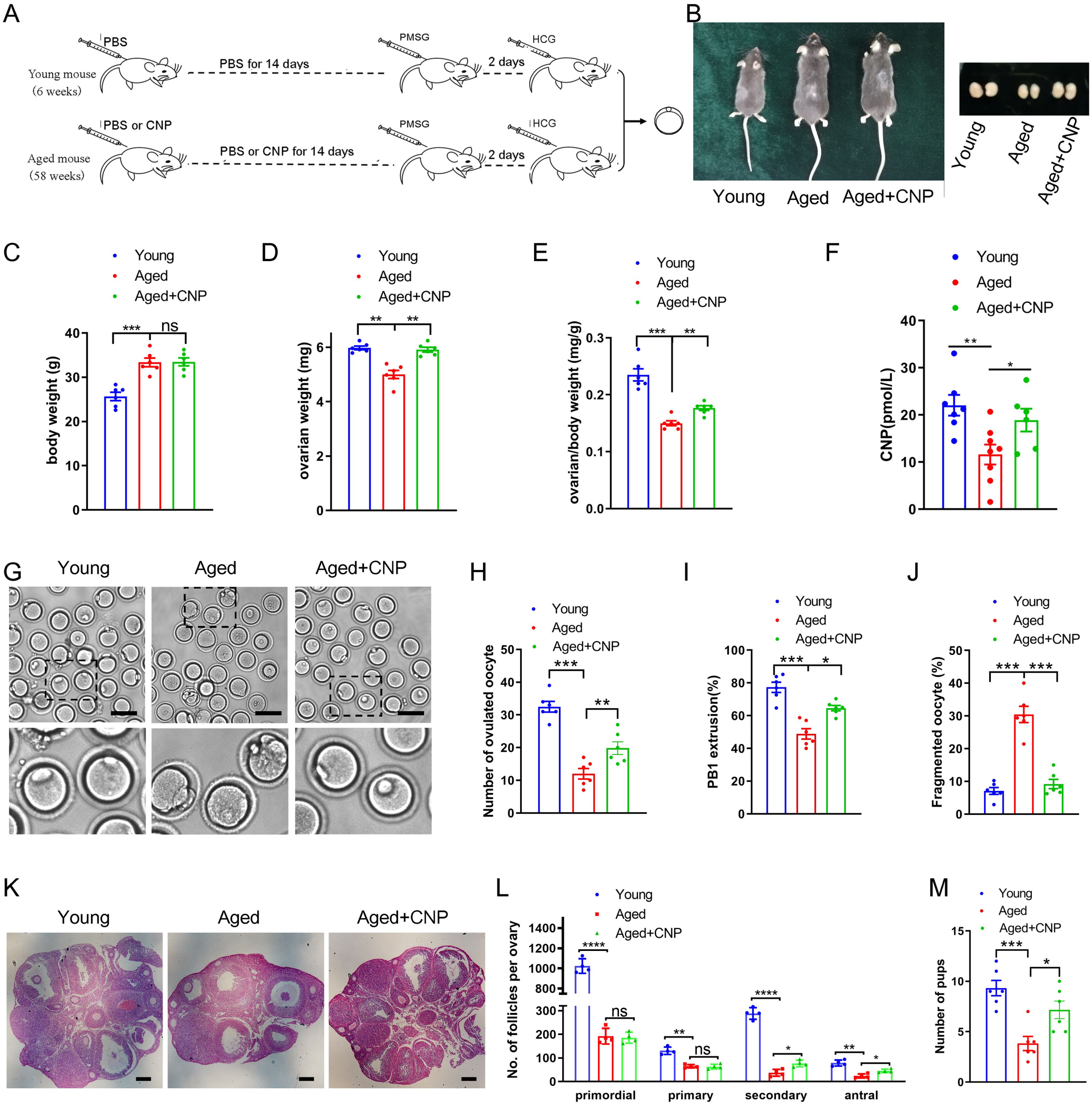
A
PBS
Young mouse
(6 weeks)
PBS for 14 days
PMSG
2 days
HCG
PBS or CNP
Aged mouse
(58 weeks)
PBS or CNP for 14 days
PMSG
2 days
HCG
B
Young
Aged
Aged+CNP
Young
Aged
Aged+CNP
C
Young
Aged
Aged+CNP
body weight (g)
***
ns
D
Young
Aged
Aged+CNP
ovarian weight (mg)
**
**
E
Young
Aged
Aged+CNP
ovarian/body weight (mg/g)
***
**
F
Young
Aged
Aged+CNP
CNP(pmol/L)
**
*
G
Young
Aged
Aged+CNP
H
Young
Aged
Aged+CNP
Number of ovulated oocyte
***
**
I
Young
Aged
Aged+CNP
PB1 extrusion(%)
***
*
J
Young
Aged
Aged+CNP
Fragmented oocyte (%)
***
***
K
Young
Aged
Aged+CNP
L
Young
Aged
Aged+CNP
No. of follicles per ovary
****
ns
**
ns
****
*
**
*
primordial
primary
secondary
antral
M
Young
Aged
Aged+CNP
Number of pups
***
*

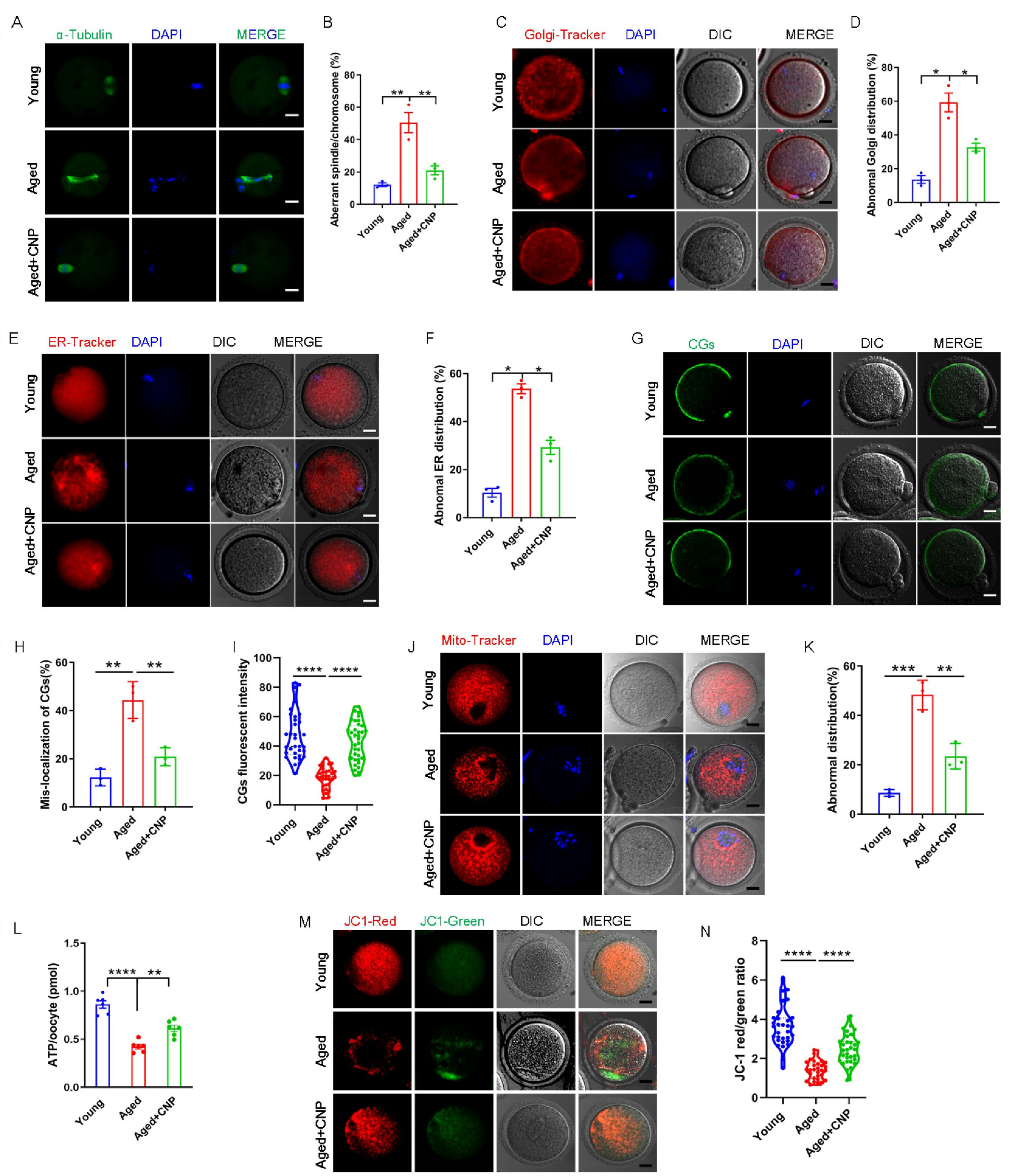
A
α-Tubulin
DAPI
MERGE
Young
Aged
Aged+CNP
B
Aberrant spindle/chromosome (%)
Young
Aged
Aged+CNP
C
Golgi-Tracker
DAPI
DIC
MERGE
D
Abnomal Golgi distribution (%)
E
ER-Tracker
F
Abnomal ER distribution (%)
G
CGs
H
Mis-localization of CGs(%)
I
CGs fluorescent intensity
J
Mito-Tracker
K
Abnormal distribution(%)
L
ATP/oocyte (pmol)
M
JC1-Red
JC1-Green
N
JC-1 red/green ratio

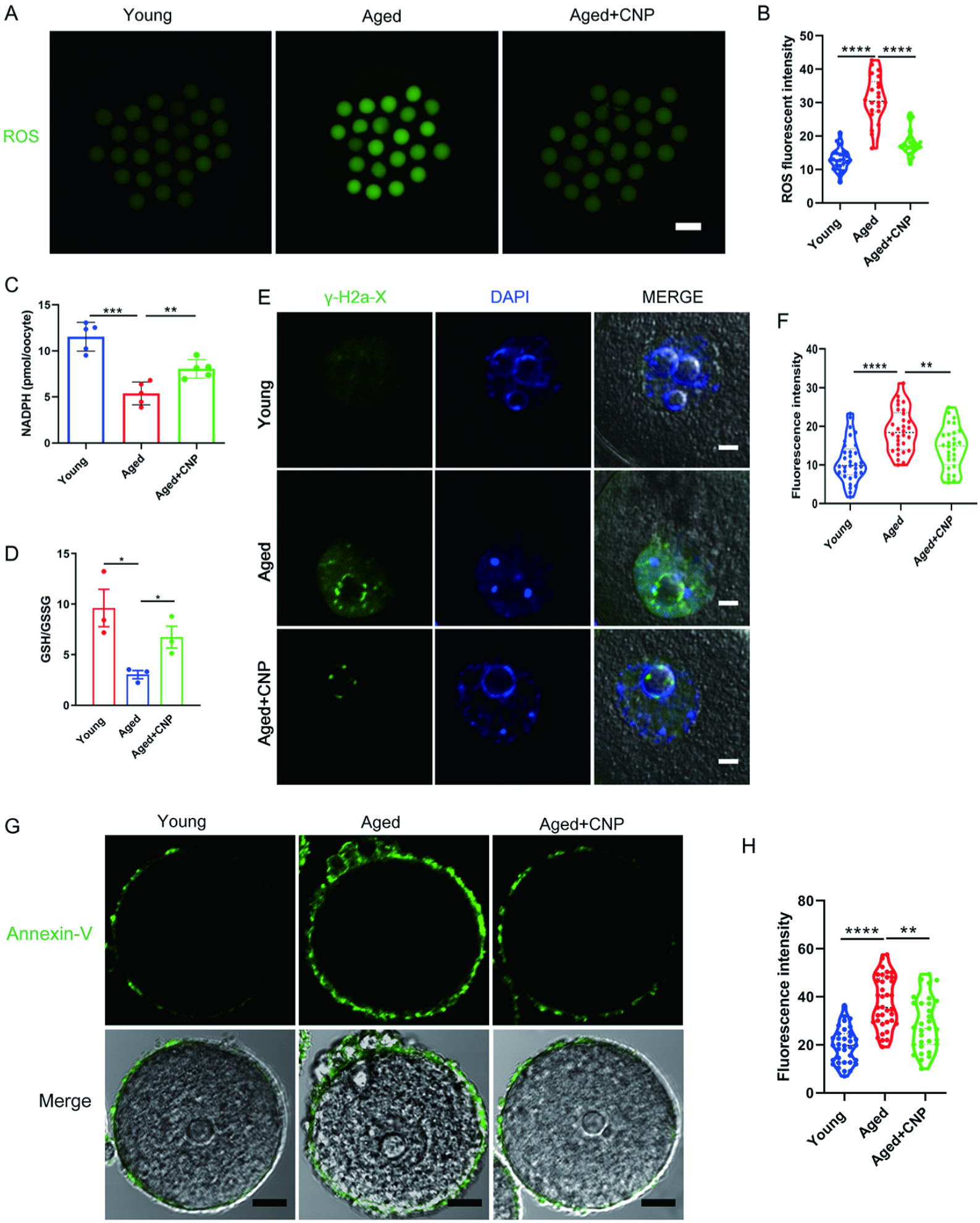
A
Young
Aged
Aged+CNP
ROS
B
ROS fluorescent intensity
****
****
Young
Aged
Aged+CNP
C
NADPH (pmol/oocyte)
***
**
Young
Aged
Aged+CNP
D
GSH/GSSG
*
*
Young
Aged
Aged+CNP
E
γ-H2a-X
DAPI
MERGE
Young
Aged
Aged+CNP
F
Fluorescence intensity
****
**
Young
Aged
Aged+CNP
G
Young
Aged
Aged+CNP
Annexin-V
Merge
H
Fluorescence intensity
****
**
Young
Aged
Aged+CNP

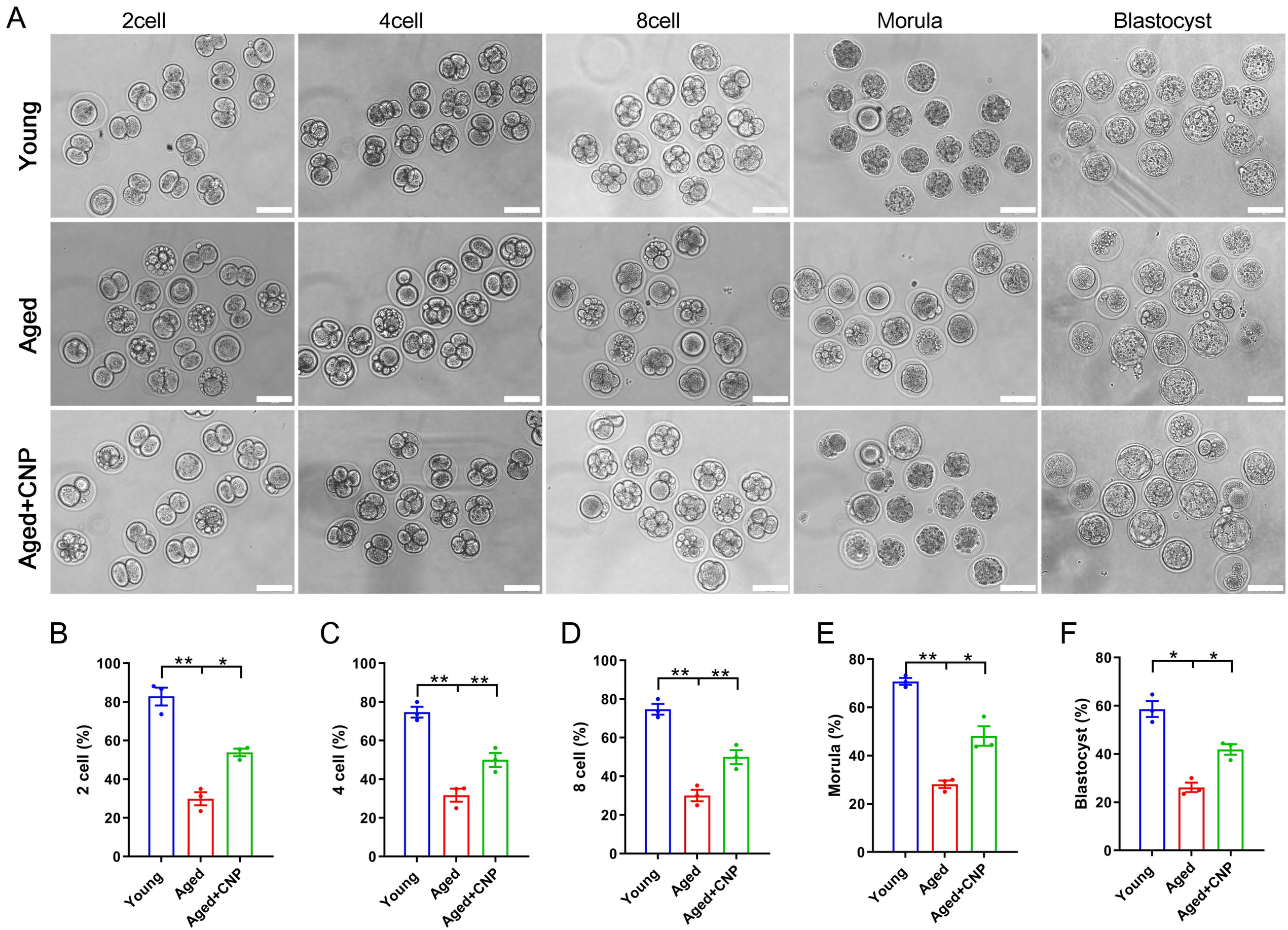
A
2cell
4cell
8cell
Morula
Blastocyst
Young
Aged
Aged+CNP
B
2 cell (%)
C
4 cell (%)
D
8 cell (%)
E
Morula (%)
F
Blastocyst (%)
Young
Aged
Aged+CNP
**
*

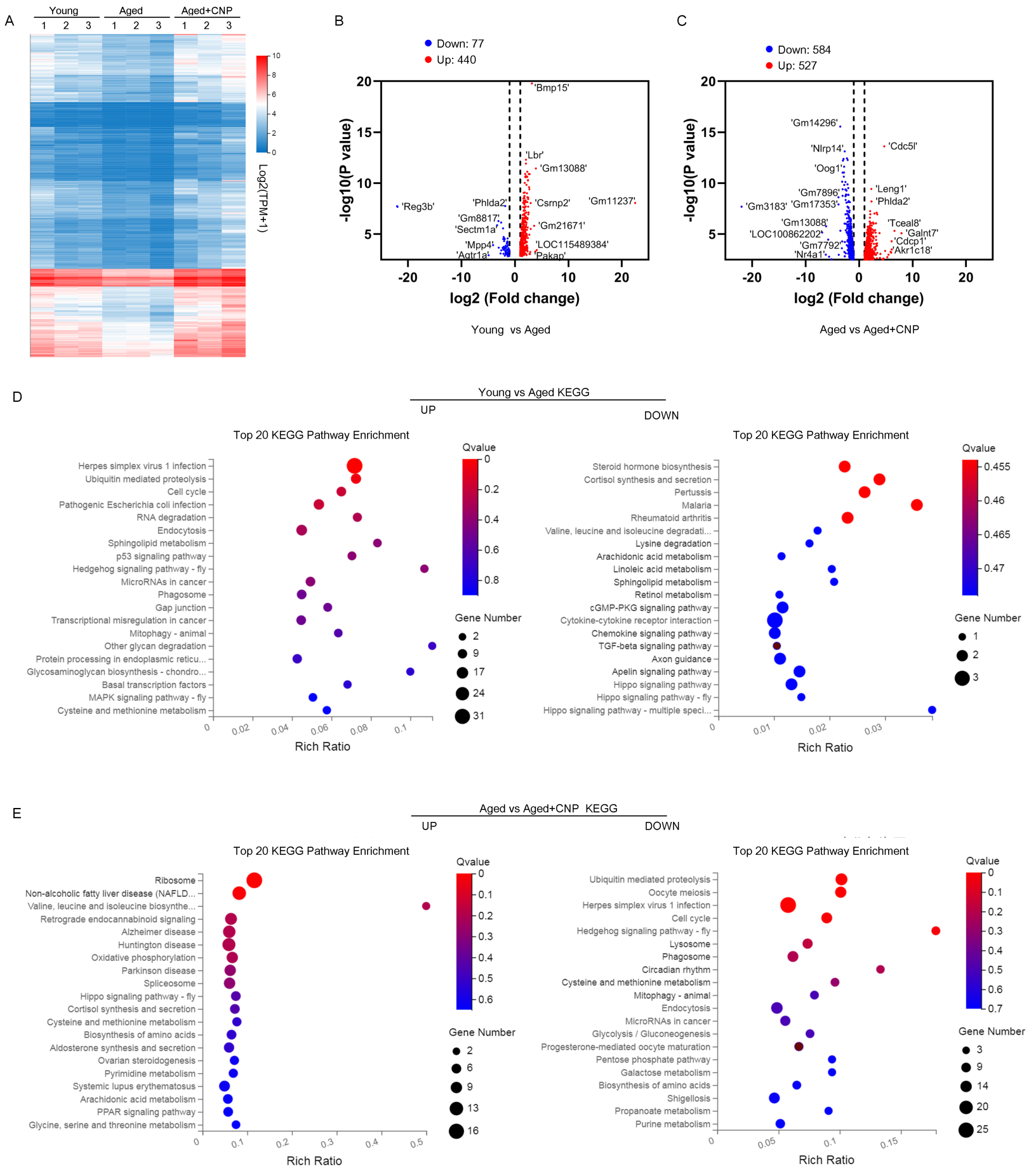
A
Young
Aged
Aged+CNP
1 2 3 1 2 3 1 2 3
Log2(TPM+1)
B
Down: 77
Up: 440
-log10(P value)
log2 (Fold change)
'Bmp15'
'Lbr'
'Gm13088'
'Reg3b'
'Phlda2'
'Csrnp2'
'Gm11237'
'Gm8817'
'Sectm1a'
'Gm21671'
'Mpp4'
'Agtr1a'
'LOC115489384'
'Pakap'
Young vs Aged
C
Down: 584
Up: 527
'Gm14296'
'Nlrp14'
'Cdc5l'
'Oog1'
'Gm7896'
'Leng1'
'Gm3183'
'Gm17353'
'Phlda2'
'Gm13088'
'Tceal8'
'LOC100862202'
'Galnt7'
'Cdcp1'
'Gm7792'
'Akr1c18'
'Nr4a1'
Aged vs Aged+CNP
D
Young vs Aged KEGG
UP
DOWN
Top 20 KEGG Pathway Enrichment
Herpes simplex virus 1 infection
Ubiquitin mediated proteolysis
Cell cycle
Pathogenic Escherichia coli infection
RNA degradation
Endocytosis
Sphingolipid metabolism
p53 signaling pathway
Hedgehog signaling pathway - fly
MicroRNAs in cancer
Phagosome
Gap junction
Transcriptional misregulation in cancer
Mitophagy - animal
Other glycan degradation
Protein processing in endoplasmic reticu...
Glycosaminoglycan biosynthesis - chondro...
Basal transcription factors
MAPK signaling pathway - fly
Cysteine and methionine metabolism
Rich Ratio
Qvalue
Gene Number
Top 20 KEGG Pathway Enrichment
Steroid hormone biosynthesis
Cortisol synthesis and secretion
Pertussis
Malaria
Rheumatoid arthritis
Valine, leucine and isoleucine degradati...
Lysine degradation
Arachidonic acid metabolism
Linoleic acid metabolism
Sphingolipid metabolism
Retinol metabolism
cGMP-PKG signaling pathway
Cytokine-cytokine receptor interaction
Chemokine signaling pathway
TGF-beta signaling pathway
Axon guidance
Apelin signaling pathway
Hippo signaling pathway
Hippo signaling pathway - fly
Hippo signaling pathway - multiple speci...
Rich Ratio
Qvalue
Gene Number
E
Aged vs Aged+CNP KEGG
UP
DOWN
Top 20 KEGG Pathway Enrichment
Ribosome
Non-alcoholic fatty liver disease (NAFLD...
Valine, leucine and isoleucine biosynthe...
Retrograde endocannabinoid signaling
Alzheimer disease
Huntington disease
Oxidative phosphorylation
Parkinson disease
Spliceosome
Hippo signaling pathway - fly
Cortisol synthesis and secretion
Cysteine and methionine metabolism
Biosynthesis of amino acids
Aldosterone synthesis and secretion
Ovarian steroidogenesis
Pyrimidine metabolism
Systemic lupus erythematosus
Arachidonic acid metabolism
PPAR signaling pathway
Glycine, serine and threonine metabolism
Rich Ratio
Qvalue
Gene Number
Top 20 KEGG Pathway Enrichment
Ubiquitin mediated proteolysis
Oocyte meiosis
Herpes simplex virus 1 infection
Cell cycle
Hedgehog signaling pathway - fly
Lysosome
Phagosome
Circadian rhythm
Cysteine and methionine metabolism
Mitophagy - animal
Endocytosis
MicroRNAs in cancer
Glycolysis / Gluconeogenesis
Progesterone-mediated oocyte maturation
Pentose phosphate pathway
Galactose metabolism
Biosynthesis of amino acids
Shigellosis
Propanoate metabolism
Purine metabolism
Rich Ratio
Qvalue
Gene Number

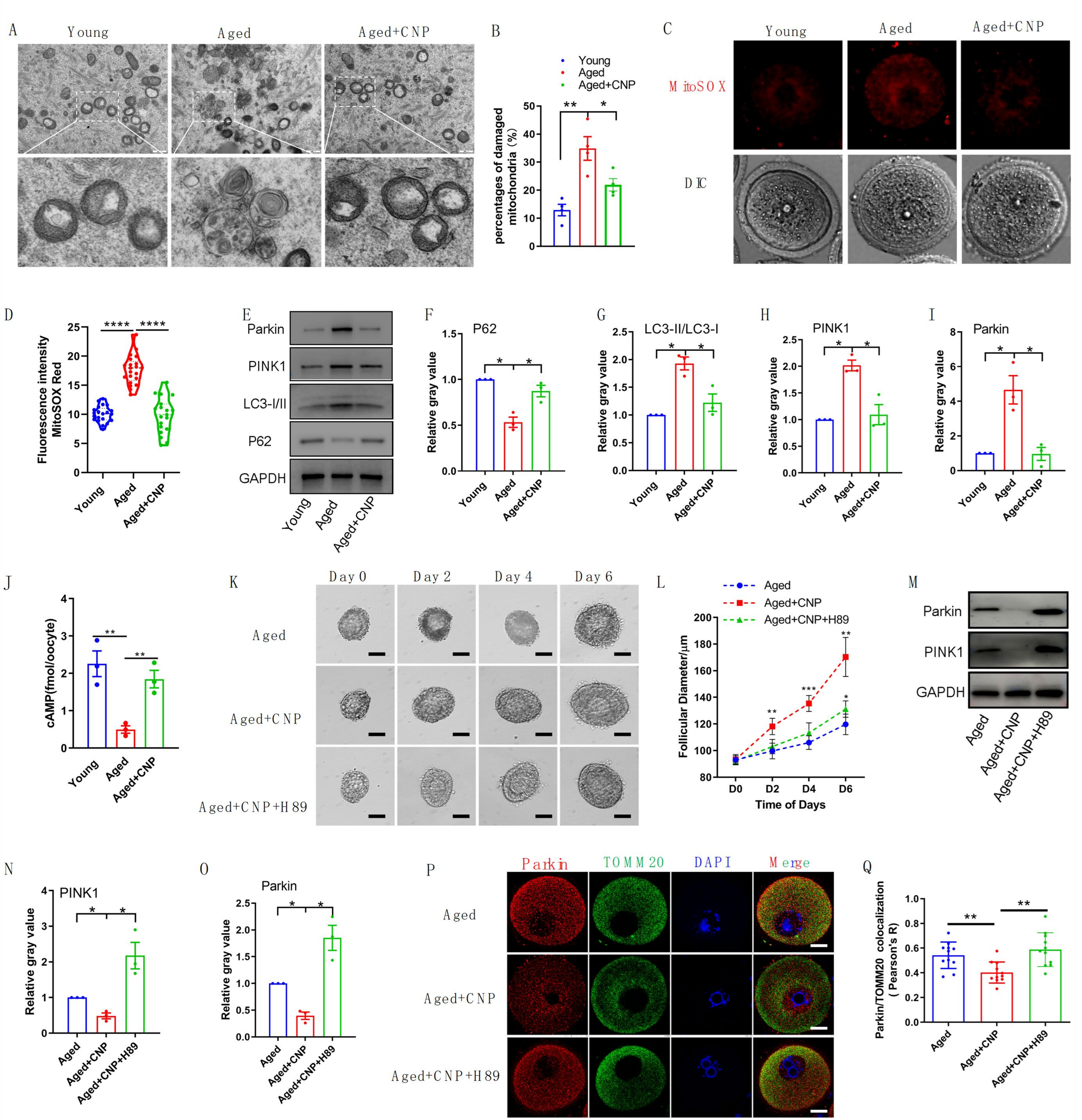
A
Young
Aged
Aged+CNP
B
Young
Aged
Aged+CNP
percentages of damaged mitochondria (%)
C
Young
Aged
Aged+CNP
MitoSOX
DIC
D
Fluorescence intensity MitoSOX Red
Young
Aged
Aged+CNP
E
Parkin
PINK1
LC3-I/II
P62
GAPDH
Young
Aged
Aged+CNP
F
P62
Relative gray value
Young
Aged
Aged+CNP
G
LC3-II/LC3-I
Relative gray value
Young
Aged
Aged+CNP
H
PINK1
Relative gray value
Young
Aged
Aged+CNP
I
Parkin
Relative gray value
Young
Aged
Aged+CNP
J
cAMP(fmol/oocyte)
Young
Aged
Aged+CNP
K
Day 0
Day 2
Day 4
Day 6
Aged
Aged+CNP
Aged+CNP+H89
L
Aged
Aged+CNP
Aged+CNP+H89
Follicular Diameter/μm
D0
D2
D4
D6
Time of Days
M
Parkin
PINK1
GAPDH
Aged
Aged+CNP
Aged+CNP+H89
N
PINK1
Relative gray value
Aged
Aged+CNP
Aged+CNP+H89
O
Parkin
Relative gray value
Aged
Aged+CNP
Aged+CNP+H89
P
Parkin
TOMM20
DAPI
Merge
Aged
Aged+CNP
Aged+CNP+H89
Q
Parkin/TOMM20 colocalization (Pearson's R)
Aged
Aged+CNP
Aged+CNP+H89